Recovery of Isostatic Topography over North America from Topographic and CHAMP Gravity Correlations

Laramie V. Potts[1] C. K. Shum[1], Ralph von Frese[2], Shin-Chan Han[1], and Rainer Mautz[1,3]

[1] Laboratory for Space Geodesy and Remote Sensing, Ohio State University, Columbus, USA *(potts.3@osu.edu)*
[2] Dept. of Geological Sciences, Ohio State University, Columbus, USA.
[3] Institute of Astronomical, Physical and Mathematical Geodesy, Technical University of Berlin, Germany.

Summary. We investigate North American crustal structure and mass loads from spectral correlation analysis of topographic, CHAMP and terrestrial gravity data. We use free-air and terrain gravity correlations to isolate tectonically driven vertical motions and mass imbalances of the crust and lithosphere. Specifically, we apply correlation filters to decompose the free-air gravity anomalies into terrain-correlated and terrain-decorrelated components to yield compensated terrain gravity effects that we evaluate for crustal thickness variations. Our results compare quite favourably with the seismically inferred global crustal thickness model Crust5.1 and a 3.4 km rms difference with LITH5.0 over North America. Terrain-correlated anomalies reveal mass excesses and deficits that are interpreted as uncompensated elements of the crust. For Hudson Bay, the average terrain-correlated free-air anomaly suggests that the crustal topography is depressed by about 400 m. Because glacial isostatic adjustment considerations can only marginally account for the depression, we speculate that it may reflect other effects such as a preglacial impact.

Key words: crustal thickness, correlations, gravity, topography, Hudson Bay

1 Introduction

Crustal modeling plays an important role in the prediction of isostatic surface topography, which is defined as the large-scale background topography that is in equilibrium at the surface of the Earth [1]. Non-zero free-air gravity anomalies over North America indicate lateral variations of uncompensated masses in the subsurface. In the mantle, these lateral density variations can reflect convective flows that generate vertical stresses at the base of the lithosphere, which by traction can sustain the observed topography as uncompensated crustal mass (e.g., [6]). Hence, the observed topography can involve superposed isostatic and dynamic topography contributions.

Seismic refraction and geodynamic modeling commonly provide regional characterizations of the isostatic and dynamic components of topography [1].

Specifically, analyses of the global Crust5.1 model of $5^0 \times 5^0$ crustal thickness variations [8] and the regional Canadian LITH5.0 crustal thickness model [10] suggest that most of the cratonic regions of North America lie at lower elevations than predicted by crustal isostasy. By subtracting the isostatic topography from the observed topography, dynamic topography is revealed that may constrain mantle flow. However, these complex seismic-geodynamic long wavelength flow models (e.g., [1]; [9]; [11]) overpredict by 25% the dynamic topography amplitudes [6]. These dynamic topography estimates may be limited by subjective choices of boundary conditions and depth-dependent profiles of mantle viscosity (e.g., [5]), sparseness of seismic stations, and uncertainties associated with densities of crustal layers (e.g., [1]; [8]; [10]).

Gravity data comprise the intergrated effects of uncompensated mass loads from the core to the crust. For example, the observed gravity anomaly minimum over Hudson Bay has been attributed to glacial isostatic adjustment (GIA) and mantle convection (e.g., [1]; [7]; [9]; [11]). However, topography data provide useful constraints to account for the gravity effects of crustal loads. Spectral correlation analysis between free-air and topographic gravity effects provide additional constraints on the lithosphere by extracting patterns of uncompensated mass variations [12]. The focus of this paper is to study constraints on dynamic and isostatic topography over North America from the joint analysis of gravity and topography data.

2 Gravity crustal modeling

Figure 1.a shows free-air gravity anomalies of North America evaluated at 20 km altitude from the TEG4 gravity model complete to degree 200 [3]. This model combines CHAMP terrestrial gravity data for the best estimate currently available of the free-air gravity anomalies at 20 km altitude (e.g., [15] this volume).

Figure 1.b shows the topography model from ETOPO5. The gravity effect of the terrain in Figure 1.c sums the contributions from the ice, water, and rock components assuming constant density values in each layer of 0.917 g/cm^3, 1.028 g/cm^3, and 2.8 g/cm^3, respectively (e.g., [1]). We conduct our analysis at 20-km altitude to minimize the effects from local terrain density and elevation errors. Dominated by rock topography, the terrain gravity effect is about five times larger than the poorly correlated (CC=0.2) free-air anomalies.

We separate the terrain-correlated and -decorrelated components of the free-air gravity anomalies on the basis of the correlation spectrum that we obtained from the Fourier transforms of the free-air (Figure 1.a) and terrain gravity effects (Figure 1.b) [14]. Inversely transforming the wavenumber components of the free-air anomalies that were strongly correlated both positively (CC(k) $\geq$ 0.6) and negatively (CC(k) $\leq$ -0.6) with the wavenumber components of the terrain gravity effects, determines the terrain-correlated

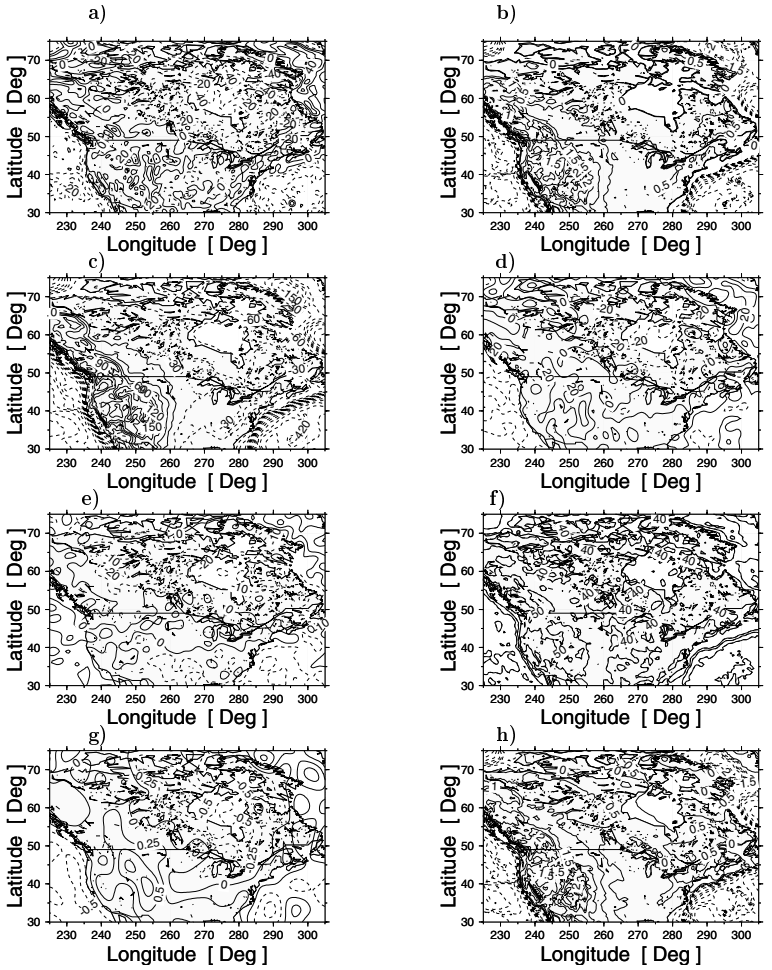

Fig. 1. Crustal modeling using TEG-4 free-air gravity anomalies (a) and topography (b). Terrain gravity effects (c) are the integerated effects of ice, water and rock. Free-air gravity components are divided in terrain-correlated (d) and terrain-decorrelated (e) anomalies. The modeling yields estimates of crustal thickness variations (f), dynamic topography (g), and isostatic topography (h).

free-air anomalies shown in Figure 1.d. The correlation coefficient cutoff values (CC(k)) for passing the k-th wavenumber component were chosen to nullify the correlation between the compensated terrain gravity effects (not shown) and the terrain-decorrelated free-air anomalies in Figure 1.e.

Subtracting the terrain-correlated components from the free-air anomalies yields the terrain-decorrelated free-air components. The longer wavelength components may best reveal the effects deep subcrustal mass variations related to deep mantle flow because of the abscence of the relatively strong

interfering long wavelength free-air anomalies from uncompensated crustal terrain [12]. The higher frequency components can also reflect uncompensated density variations within the crust [12], but these signals are typically close to the noise level of the gravity data.

For estimating Moho and related crustal thickness variations of North America, we subtract the terrain-correlated free-air anomalies (Figure 1.d) from the terrain gravity effects (Figure 1.b) for the compensated terrain gravity effects. The lack of compensated terrain effects in the free-air anomalies reflects annihilating signals that may be analyzed for Moho variations in the context of an appropriate compensation model. Reversing the polarities of the compensated terrain effects yields the annihilating signals for obtaining Moho estimates by spherical coordinate inversions using Gauss-Legendre quadrature integration. The inversions estimated the thicknesses of spherical prisms about a reference depth of 30 km below mean sea level assuming a 0.5 g/cm^3 density contrast for the mantle relative to the crust (e.g., [1]). Our crustal thickness model, referenced to the EGM96 geoid, compares quite favourably with Crust5.1. Relative to LITH5.0, our results have a rms difference of 3.4 km over mid-latitudes which is well within the acceptable error limits of the seismically-inferred thicknesses [10]. At high latitudes where seismic observations are relatively sparse, our model over-estimates seismic crustal thickness estimates by about 15%.

Assuming that the terrain-correlated free-air anomalies reflect mostly uncompensated crustal topography, the inversion of these anomalies about the surface topography with a density contrast of 2.8 g/cm^3 furnishes the dynamic topography in Figure 1.g. Subtracting Figure 1.g from Figure 1.b yields the isostatic topography in Figure 1.h. The gravity effect from the dynamic topography matches in a least-squares sense the terrain-correlated free-air gravity anomalies of Figure 1.d. The crust presumably is attempting to achieve isostatic equilibrium and a zero-mean free-air gravity anomaly. Hence, where the dynamic topography is above (positive) or below (negative) the observed topography, the crust may be under pressure to subside or rise, respectively.

3 Hudson Bay Results

For Hudson Bay, the mean isostatic topography estimated in Figure 1.h is about 420 m higher than the observed topography so that the crust is in isostatic uplift. Absolute gravity measurements over a twelve year period near Hudson Bay show an average decrease in gravity of about ± 0.2 μGals/yr which corresponds to ± 1.3 mm/yr uplift [4]. Vertical crustal motion over Hudson Bay has been attributed to the visco-elastic response of the lithosphere to the load of the Laurentide ice sheet that covered northern North America for thousands of years until its retreat some 10,000 years ago [7]. Present models on Laurentide deglaciation that satisfy uplift data predict

only 15% to 30% of the observed -50 mGal free-air gravity anomaly [2] while geodynamic models attribute up to 50% of the total long wavelength geoid to GIA (e.g., [9]; [11]; [13]), depending on the choice of model parameters [5]. Assuming the crust was in isostatic equilibrium prior to ice loading, the -50 mGal gravity anomaly accomodates a surface depression of about 1.7 km due to ice loading (assuming the infinite-slab approximation) that promotes in turn problematic mantle viscosity and lithosphere thickness estimates (e.g., [2]). However, the terrain-correlated anomalies (Figure 1.d) represent about 70% of the original free-air anomaly signal (Figure 1.a) suggesting that the topographic deficit explains a significant percentage of the negative free-air gravity anomaly. Hence, the gravity effect of uncompensated crustal loads accounts for more than half of the observed gravity. The terrain-correlated free-air anomalies thus may mostly reflect other isostatic contributions than those due to GIA.

The terrain-decorrelated free-air gravity components (Figure 1.e) were assumed to not contribute to dynamic surface topography, but rather to arise from lateral subcrustal density variations. Seismic velocity data indicate that North America may lie above an anomalously cold, dense region that acts to depress the surface (e.g., [5]; [6]). Deep mantle convective flows may dynamically support the localized surface depression, although flow models that reconcile uplift data and gravity anomalies grossly overestimate uplift rates near Hudson Bay [7]. Hence, the terrain-decorrelated anomalies may help constrain the deep mantle flows in the context of the subcrustal density stratigraphy of Hudson Bay (e.g., [12]).

The broad dynamic topography depression centered on Hudson Bay in Figure 1.g includes a localized small central peak flanked by annuli of depressed and raised topography. The dynamic topography signature for Hudson Bay provokes the impression of a crustal impact basin. The possible location of the impact is indicated by the red triangle in Figure 1.g. The isostatic effects of the exogeneously disrupted crust dominate the terrain-correlated free-air anomalies that can only marginally be accounted for by GIA considerations. Hence, we speculate that an impact may have excavated crustal material prior to ice loading which subsequently eroded down much of the original topography of the impact basin.

4 Conclusion

We investigated topographic and gravity correlations using ETOPO5 and the TEG4 gravity model (which includes CHAMP data) at 20 km altitude to characterize possible crustal thickness variations (Figure 1.f) and related isostatic adjustments of the topography (Figure 1.g). Spectral correlation analysis decomposed the free-air anomalies (Figure 1.a) into terrain-correlated (Figure 1.d) and terrain-decorrelated (Figure 1.e) components. Terrain-correlated anomalies were interpreted mainly for dynamic surface

topography (Figure 1.g). Our analysis indicates that the terrain-correlated components represent about 70% of the total free-air gravity anomalies of North America.

The gravity minimum over Hudson Bay reflects topography undercompensated by about 400 m due possibly more to a preglacial impact or some other effect than to the retreat of the Laurentide ice sheet. The residual terrain-decorrelated free-air gravity anomalies (Figure 1.e) may constrain uncompensated mass anomalies within the crust as well as in the deeper interior where density-driven mass flows operate.

References

1. Forte A, Peltier W, Dziewonski A, Woodward R (1993) Dynamic surface topography: A new interpretation based upon mantle flow models derived from seismic tomography. Geophys Res Lett *20*: 225–228.
2. James T (1992) The Hudson Bay free-air gravity anomaly and glacial rebound. Geophys Res Lett *19(9)*: 861–864.
3. Kang Z, Bettadpur S, Tapley B, Cheng K, Ries J (2003) Determination of CHAMP accelerometer calibration parameters. In: Reigber Ch, Luehr J, Schwintzer P (eds.), First CHAMP Mission Results for Gravity, Magnetics, and Atmospheric Studies. Springer-Verlag: 19–25.
4. Lambert A, Courtier N, Sasagawa G, Klopping F, Winester D, James T, and Liard J (2001) New constraints on Laurentide postglacial rebound from absolute gravity measurements. Geophy Res Lett *28(10)*: 2109–2112.
5. Li A, Fischer K, Wysession M, Clarke T (1998) Mantle discontinuities and temperature under the North American continental keel. Nature *395*: 160–163.
6. Lithgow-Bertelloni C, Silver P (1998) Dynamic topography, plate driving forces and the African superswell. Nature *395*: 269–272.
7. Mitrovica J (1997) Going halves over Hudson Bay. Nature *390*: 444–446.
8. Mooney W, Laske G, Masters T (1998) CRUST5.1: A global crustal model at $5^0 \times 5^0$. J Geophys Res *103*: 727–747.
9. Pari G, Peltier W (2000) Subcontinental mantle dynamics: A further analysis based on the joint constraints of dynamic surface topography and free-air gravity. J Geophys Res *105*: 5635–5662.
10. Perry H, Eaton D, Forte A (2002) LITH5.0: A revised crustal model for Canada based on Lithoprobe results. Geophys J Int *150*: 285–294.
11. Perry H, Forte A, Eaton D (2003) Upper-mantle thermochemical structure below North America from seismic-geodynamic flow models. Geophys J Int *154*: 279–299.
12. Potts L, von Frese R (2003) Lunar subcrustal mass differentiation from spectral free-air and terrain gravity correlations. J Geophys Res *108(E4)*: 10.1029/2000JE001440.
13. Simons M, Hager B (1997) Localization of the gravity field and the signature of glacial rebound. Nature *390*: 500–504.
14. von Frese R, Jones M, Kim J, Li W (1997) Spectral correlation of magnetic and gravity anomalies of Ohio. Geophys *62(1)*: 365–380.
15. von Frese R, Kim H, Taylor P, Asgharzadeh M (2003) Reliability of CHAMP anomaly contributions. this volume.